Capturing the Mesoarchean Emergence of Continental Crust in the Coorg Block, Southern India

Nick M W Roberts[1*], M Santosh[2,3,4]

[1]NERC Isotope Geosciences Laboratory, British Geological Survey, Nottingham, NG12 5GG, UK

[2]School of Earth Sciences and Resources, China University of Geosciences Beijing, 29 Xueyuan Road, Beijing 100083, China

[3]Centre for Tectonics, Exploration and Research, University of Adelaide, Adelaide, SA 5005, Australia

[4]Department of Geology, Northwest University, Northern Taibai Str. 229, Xi'an 710069, China

*corresponding author: nirob@bgs.ac.uk

Words: 3499

Figures: 5

Tables: 0

References: 55

Supplementary Files: 3

Key Points:

Zircon U-Pb-Hf-O isotope dataset from the Coorg Block, Southern India, representing three phases of magmatism from ca. 3.5 to ca. 3.1 Ga.

Increasing oxygen isotope values through time record an increase in sediment recycling, and continental thickening and emergence above sea-level.

This article has been accepted for publication and undergone full peer review but has not been through the copyediting, typesetting, pagination and proofreading process which may lead to differences between this version and the Version of Record. Please cite this article as doi: 10.1029/2018GL078114

We relate maturation of the continental crust as it thickens and emerges above sea-level to the increasing strength of the lithosphere

Abstract

The emergence of Earth's continental crust above sea-level is debated. To assess whether emergence can be observed at a regional scale, we present zircon U-Pb-Hf-O isotope data from magmatic rocks of the Coorg Block, southern India. A 3.5 Ga granodiorite records the earliest felsic crust in the region. Younger phases of magmatism at 3.37-3.27 Ga and 3.19-3.14 Ga, comprising both reworked crust and juvenile material, record successive crustal maturation. We interpret an elevation in $\delta^{18}O$ through time as an increase in both the amount of sediment recycling, and hence, crustal thickening, as well as an increase in the emerged area of continental crust available for weathering. Geochemical signatures do not point to any apparent change in geodynamic regime. We interpret the isotopic evolution of these rocks as solely reflecting regional emergence and thickening of the continental crust, assisted by the increasing strength of the lithosphere.

1. Introduction

There is continuing debate over both the onset of modern-day-style plate tectonics and the emergence of continental crust above sea level. The onset of modern-day-style plate tectonics, has been long-debated. Estimates range from the Hadean (Harrison, 2009) to the Neoproterozoic (Stern, 2008), but many occur in the range of 3.2 to 2.5 Ga (see Hawkesworth et al., 2018; Roberts and Spencer, 2015). Although it is common to quote a single age as a transitional point in Earth evolution, e.g. 3.0 Ga (Dhuime et al., 2012), it is more likely that the gradual secular cooling in mantle temperatures may have led to a protracted transition from pre-plate tectonic to plate tectonic geodynamic regimes (Condie, 2016; Spencer et al., 2017). Similarly, the emergence of large areas of continental crust above sea-level is also predicted to occur around the late Archean, based on both numerical models (Flament et al, 2008; Vlaar, 2000), and geochemical evidence (Pons et al., 2013; Szilas et al., 2016). However, numerical models for continental emergence are built on several wide-ranging assumptions such as Earth's thermal evolution and continental crustal

growth rate and have wide-ranging estimates from the Hadean to the Neoproterozoic (Maruyama and Ebisuzaki, 2017; Lee et al., 2018).

Our knowledge of early Earth geodynamics has been significantly improved through the advent of complex numerical models (e.g. Fischer and Gerya, 2016; Rozel et al., 2017; Sizova et al., 2011); however, these models require ground-truthing within the limited rock record. There are several cratons which preserve Earth's Eoarchean to Mesoarchean geological history, and these indicate that both subduction-dominated and plume-dominated processes occurred from at least the Mesoarchean, with different cratons being dominated by different settings (e.g. Van Kranendonk, 2010). Detrital mineral records provide an important archive of the continental crust, but removal from their source means they lack accompanying geochemical and geophysical constraints. Here, we present a combined U-Pb-Hf-O zircon isotope dataset of Palaeoarchean to Mesoarchean magmatic rocks from the Coorg Block of southern India. We interpret a systematic increase in zircon $\delta^{18}O_{VMSOW}$ through time, coincident with an increasing range in zircon $^{176}Hf/^{177}Hf_i$ and Th/U ratios, as reflecting a combination of a regional increase in the area of continental emergence and of increasing crustal thickening and burial, from 3.5 to 3.1 Ga.

2. Geological Setting

Southern India hosts a belt of crustal blocks that represent an arc accretionary belt formed during the Mesoarchean to Neoarchaen (Jayananda et al., 2015, 2018; Peucat et al., 2015; Santosh et al., 2015, 2016), and accreted to the Dharwar Craton at ca. 2.5 Ga. The Coorg Block, the north-westernmost arc terrane, comprises the oldest known rocks from this belt, it therefore provides an ideal locality to study early crust formation. The Coorg block is dominated by upper amphibolite to granulite-facies charnockite and tonalite-trondhjemite-granodiorite gneisses (TTGs), but also contains less abundant mafic-ultramafic rocks, now in the form of tremolite-actinolite schists (Santosh et al., 2015, 2016). Metasediments are rare within the core of the block, but are found as tens of metre thick bands of khondalites (granulite-facies metapelites) along its periphery; these are younger than the magmatic

rocks based upon their detrital zircon ages (Santosh et al., 2016). Based on the lithological and geochemical characteristics, Santosh et al. (2015, 2016) interpret the block to represent the mid-crust of a continental arc.

3. Samples and methods

Seven metaigneous samples previously described by Santosh et al. (2015, 2016) were selected for detailed work. Zircon was analysed in the following order, oxygen isotopes (Institute of Geology and Geophysics, Chinese Academy of Sciences, Beijing), U-Pb isotopes (Natural Environment Research Council (NERC) Isotope Geosciences Laboratory (NIGL), Nottingham), and Lu-Hf isotopes (NIGL). Detailed methods and the dataset are located in the supplementary online material (Fielding et al., 2018; Horstwood et al., 2016; Li et al., 2010a, 2010b; Spencer et al., 2014).

4. Results

4.1 U-Pb Geochronology

Crystallization ages of the seven samples range from ca. 3502 to 3140 Ma, overlapping those previously obtained by Santosh et al. (2015, 2016). We split the samples into Phase 1, comprising a 3502 Ma granodiorite gneiss; Phase 2, comprising three samples from ca. 3.37 to 3.27 Ga (charnockite and granodiorite); and Phase 3, comprising three samples at ca. 3.19 to 3.14 Ga (charnockite and a meta-tuff). Isotope data are plotted with individual $^{207}Pb/^{206}Pb$ ages, since the LA-ICP-MS method lacks resolution at this age range to confidently determine magmatic, anticrystic and xenocrystic zircons, and to derive a precise crystallisation age of each unit. ZirconTh/U ratios are shown in Figure 2a. Although the discriminator of magmatic versus metamorphic zircon is arbitrary and not always accurate (Rubatto, 2017), the data show a general trend of an increasing range of Th/U values through time, importantly with a larger population of low Th/U zircon domains (metamorphic) within Phase 3 magmatism.

4.2 Lu-Hf isotopes

Hf isotope data are plotted in Figure 2b as initial age-corrected $^{176}Hf/^{177}Hf$ ratio ($^{176}Hf/^{177}Hf_i$) versus $^{207}Pb/^{206}Pb$ age. For comparison, also shown are evolution trends of Lu/Hf = 0, 0.012

and 0.029. The horizontal evolution (Lu/Hf = 0) is equivalent to lead-loss. The trend of Lu/Hf = 0.012 corresponds to the estimated value of average mafic TTG-forming crust (Gardiner et al., 2018). The trend of Lu/Hf = 0.029 corresponds to the value required to produce the most radiogenic values of Phase 2 and 3 magmatism from a source equivalent to the average of Phase 1.

The oldest sample (Phase 1) represents juvenile magmatism with an average $^{176}Hf/^{177}Hf_i$ of 0.28062. Younger zircon domains in this sample likely reflect lead-loss during subsequent magmatic phases. This sample represents the earliest formed felsic crustal component, derived directly or through a multi-stage melt-differentiation process from the earliest formed mafic proto-crust. Of Phase 2 magmatism, the ca. 3.37 Ga rocks were derived mostly from reworking of the early formed proto-crust, assuming a composition similar to Phase 1 magmatism with a Lu/Hf around 0.012. The 3.27 Ga sample is likely recording renewed juvenile magmatic addition since it lies at a higher $^{176}Hf/^{177}Hf_i$. Phase 3 magmatism may also represent reworking of the earliest formed 3.5 Ga proto-crust, if such crust is mafic in composition with a high Lu/Hf ratio. However, most data plot above the evolution trend displayed (Lu/Hf = 0.012), and therefore reflect some juvenile input to the crust at this time. A spread in $^{176}Hf/^{177}Hf_i$ equivalent to ten epsilon units across individual Phase 3 samples likely reflects mixed crust-mantle magmatism, although disequilibrium melt processes cannot be excluded (e.g. Tang et al., 2014; Wang et al., 2018). Data from previous studies of these and other samples from the Coorg Block (see Fig. 2b) overlap those presented here, although with slightly larger scatter.

We calculated simple two-component mixture modelling to provide an indication of the potential mantle contributions through time. A full description of the end-member compositions and results are given in the supplementary information. We assume that Phase 1 presents mantle-derived magmatism, although it is not constrained whether the first mafic protolith that melted to form this granodiorite was extracted around the crystallisation age of ca. 3.5 Ga, or earlier (the two-stage Hf model age is 3.8 Ga). The juvenile Phase 2 sample (PKD-1) corresponds to a mixture of 50% depleted mantle and 50% Phase 1 protocrust. The most juvenile Phase 3 sample (TKLD-1) requires a mixture of 37%

depleted mantle and 63% Phase 1 protocrust. The least juvenile Phase 3 sample (NDK-1) requires 15% depleted mantle.

4.3 Oxygen isotopes

Oxygen isotope data are plotted in Figure 2c as zircon $\delta^{18}O_{VMSOW}$ versus $^{207}Pb/^{206}Pb$ age, choosing only the concordant (to <10%) data. For comparison, we plot the mantle composition of +5.3±0.3‰ (Valley et al., 1998). The oldest samples fall exactly on this mantle composition, averaging +5.26‰. The next phase of magmatism (at ca. 3.37 to 3.27 Ga) records an increase in both the mean and maximum of the $\delta^{18}O_{VMSOW}$ values to +5.96 and +6.37‰, respectively. The youngest phase of magmatism records another increase in the mean and maximum to +6.28 and +6.89‰, respectively. The dashed grey line corresponds broadly to the increasing maximum values through Phase 1 to Phase 3 magmatism. Values greater than the mantle range reflect a contribution from material that has been altered at low-temperature, i.e. weathering at or near the Earth's surface (see Valley, 2003). In magmatic rocks this can be achieved by incorporation of weathered sediments to the magma source. The data presented here, at face value, therefore correspond to an increasing sedimentary component to the magmatism through time.

4.4 Geochemistry

Petrography, mineral chemistry and whole-rock geochemistry of these samples were discussed in detail in Santosh et al. (2015, 2016); notable features are their metaluminous nature, low K_2O/Na_2O ratios, enriched LREE (Light Rare Earth Elements) and LILE (Large Ion Lithophile Elements), and low Nb/Zr. These authors ascribed the rocks to typical continental arc rocks. Figure 3 presents primitive mantle (Sun & McDonough, 1989) normalised trace elements and a Quartz-Alkali Feldspar-Plagioclase classification plot; notably, all samples exhibit broadly similar LILE and LREE enrichment, and distinctive negative Nb anomalies. These characteristics are typical of magmas formed in a supra-subduction type setting; however, it is well documented that such characteristics are not exclusive, and may represent hydrous melting of mafic rocks in other settings (e.g. Johnson et al., 2017; Moyen, 2011; Moyen & Laurent, 2018; Nagel et al., 2012). The notable feature is that there is no apparent change in geochemical signature that may also reflect a change in geodynamic regime, i.e. from plume-derived to subduction derived magmas.

5. Discussion

5.1 Magma evolution

Magmatism in the Coorg Block records ca. 0.4 Gyrs of crustal evolution. We interpret the granodioritic gneiss at 3.5 Ga as representing a rare record of the earliest felsic crust formation along this entire accretionary belt. Juvenile hafnium and mantle-like oxygen isotope signatures of this sample are compatible with its formation from a mantle-derived protolith. Hf isotope data of subsequent magmatic rocks imply that this protolith formed the crustal substrate for successive periods of magmatism to be formed within and upon. A significant range in Hf isotope values for Phase 2 and 3 magmatism suggests mixed source contributions, i.e. both reworked older crust and more juvenile material. This suggests a maturing crust through time. The oxygen isotope signatures record a similar maturation through, ranging from pure mantle, to increasingly elevated signatures above the mantle average, implying an increasing sedimentary component to magmatism through time. Conversely, the geochemistry does not record any apparent change through time.

The combined zircon isotope and geochemical data lend support to a simple model involving crustal maturation through time, from early-formed mantle-derived intermediate-felsic magmatism, to later mixed crust-mantle felsic magmatism, with crust-mantle interaction and sedimentary incorporation increasing during each period of magmatism. Because the geochemical signatures do not show any marked change, we speculate that each magmatic phase is formed in a similar geodynamic regime. In concordance with the interpretation of previous studies (Santosh et al., 2015, 2016), we interpret this to be related to a subduction setting. However, we accept that subduction may have differed in its mechanics, and that crust formation and reworking in a vertically-dominated tectonic setting is also permissible (Johnson et al., 2017). To account for the evolving magmatic compositions through time, we present a unifying model below, and depicted in Figure 4.

5.2 A model of crustal maturation and continental emergence

Phase 1 of the model represents formation of the earliest felsic crust. The Phase 1 granodiorite likely formed from melting of a mafic protolith, which may have been extracted

from the mantle at 3.5 Ga or slightly earlier (<3.8 Ga). Phase 2 represents maturation into an ensialic crust (a volcanic arc?) with a range of compositions. Phase 3 represents further maturation into a thicker crust, with a potential role of crustal accretion. We interpret the oxygen isotope data to provide important constraints on emergence of this continental crust. Phase 1 lacks any sedimentary input, and is therefore compatible with submergence. Phase 2 has an increasing sedimentary component; therefore, the crust has thickened enough to allow for incorporation of sediment into the melts through burial. To produce weathered sediments in the local area, we interpret the crust as being emergent above sea-level. Phase 3 records a further increase in sedimentary incorporation, and therefore increased crustal thickening and burial. The Th/U data lend additional support to increasing tectonothermal activity during Phase 3, and this is further supported by a ca. 3.0 Ga age of metamorphism in the northern periphery of the Coorg Block, recording its accretion to Dharwar crust to the north (Amaldev et al., 2016). Such crustal-accretion tectonic processes would drive increasing sedimentary incorporation into mid- to deep-crustal magma source regions through burial. Crustal thickening during/preceding Phase 3 would also lead to further continental emergence, which would subsequently drive an increase in the $\delta^{18}O$ of the regional sedimentary volume through increased weathering.

According to our model, several parameters are evolving simultaneously: crustal thickness, continental emergence and tectonothermal activity. Crustal thickness and continental emergence are linked but not directly correlative, as they are controlled by global hypsometry. It is difficult to disentangle the signals of crustal thickness versus continental emergence from geochemistry alone. Although crustal thickness can be estimated from magma compositions (Chiaradia, 2015; Mantle and Collins, 2008; Profeta et al., 2015), this requires a large geochemical dataset, and it is unclear how applicable these correlations will be for Archean rocks.

The evolving magmatic oxygen isotope signatures could reflect changes in either one or more parameters. Firstly, the $\delta^{18}O$ signature of the sedimentary component could be static through time, in which case the data would likely reflect an increasing sedimentary contribution to each Phase of magmatism. Alternatively, the $\delta^{18}O$ signature of the sedimentary component may be increasing through time, in which case the amount of

sediment incorporated in the magmas may be static. Although it is difficult to assess this precisely, particularly without the ability to sample the sedimentary component locally, the global dataset may provide some insight. Global oxygen isotope compilations of sedimentary rocks for this period show a steady increase through time (see Figure 5a; Bindeman et al., 2016; Payne et al., 2015). Thus, the global data are compatible with more crust being weathered over time, i.e. a result of increasing continental emergence. Results of simple two component mixture modelling using the mean and maximum global shale data (Bindeman et al., 2016) are shown in Figure 5a. The results show that using either the mean or maximum, the required contribution from the sedimentary component is increasing for each Phase of magmatism (see supplementary information for details), i.e. from ca. 0 to 10.5 to 13.7% (using the maximum), or from ca. 0 to 15.5 to 21% (using the mean). We postulate that this indicates both: 1) an increasing sedimentary contribution through time, and 2) that emergence of continental crust is increasing on both the local and global scale, elevating the $\delta^{18}O$ signature of the sedimentary budget.

5.3 Global versus regional signals

Our model of Coorg Block evolution implies an increase in both crustal thickness and continental emergence in the 3.5-3.1 Ga period. This contrasts with global models based on numerical modelling of continental emergence that are younger (Neoarchean, Flament et al., 2008; Neoproterozoic, Lee et al., 2018), but is broadly correlative to models of increasing crustal thickness around 3.0 Ga (Dhuime et al., 2015). We do not constrain the area of emerged crust, but we expect it to be large enough to affect the composition of the regional sedimentary budget. To allow for the dichotomy between the numerical models cited and our results, we suggest that: 1) our data represent a regional rather than global effect, i.e. not all cratons were emergent by 3.1 Ga; and 2) crustal thickening and continental emergence are unlikely to be directly correlated across all cratons at the same time, i.e. plume-dominated and arc-dominated regions likely have differing crustal thicknesses. The global thickening of the continental crust through the Mesoarchean (e.g. Dhuime et al., 2015) may reflect an increase in a particular tectonic process (i.e. subduction); however, we suggest that this could also be the result of an increase in the strength of the lithosphere, due to decreasing mantle potential temperatures (Herzberg, 2010), so that it can support higher topography through time (Rey and Coltice, 2008).

The fact that some cratons likely formed through plume-dominated processes whereas others are dominated by arc processes (e.g. van Kranendonk, 2010) argues for heterogeneity amongst cratonic evolution. Of note, zircon oxygen isotope data supporting Mesoarchean continental emergence exist from other cratons. The Pilbara craton shows a marked increase in zircon $\delta^{18}O$ at 3.2 Ga (Van Kranendonk et al., 2015); these authors interpret this change to mark a shift in global geodynamics whereby modern-day style steep subduction and associated crustal recycling occurs after 3.2 Ga. In West Greenland, the same 3.2 Ga timeframe is also interpreted as the onset of modern accretionary style plate tectonics, based on an increase in zircon $\delta^{18}O$ and a change to wide-ranging zircon εHf - reflecting both mantle input and crustal reworking (Næraa et al., 2012). Importantly, these interpretations are different to our model, whereby we do not infer a change in (regional) geodynamics through the 3.5 to 3.1 Ga period.

Compilations of detrital zircon data with higher than mantle values through the Eo- to Neoarchean would imply that our regional data, and that of the cratons mentioned above, are not globally significant (see Figure 5b). These data would imply that significant continental reworking of altered sediments was prevalent since the dawn of the Archean (Ge et al., 2014). However, it should be noted that not all detrital data confidently represent primary values for their isotopic signatures. Oxygen isotope signatures can be modified by fluid alteration at high temperature, and this may not be recognised in all detrital datasets (Roberts et al., 2018). Some detrital datasets, particularly those form Jack Hills, have been repeated and scrutinised (e.g. Whitehouse et al., 2017), and therefore the interpretation of sedimentary incorporation is likely to have some validity (e.g. Cavosie et al., 2005). However, splitting the published data into igneous and detrital zircons for the 3.6 to 3.0 Ga time period, shows that in general, the igneous data mostly fall within the constraints recorded by the Coorg Block. We postulate that a large number of detrital data may be erroneous, either in their age assignment or their assignment of primary rather than secondary oxygen isotope values. We also note that none of the detrital data are taken from the Indian Craton, and thus there are no conflicting data from this craton itself.

In summary, our comparison of literature data for zircon oxygen isotopes from detrital and igneous rocks, highlights the need to compare the evolution of different cratons with different histories around the Earth using the magmatic record (c.f. Fisher and Vervoort, 2018). This will allow us to better constrain what timescale global changes are occurring over, and how they are represented in the global sedimentary archive. Furthermore, only by ground-truthing in the preserved rock record can we test the important constraints provided by numerical models and large detrital datasets.

6. Conclusions

Zircon U-Pb-Hf-O isotope data from the Coorg Block in southern India record evolving crust during three phases of magmatism. The earliest felsic melt recorded at ca. 3.5 Ga formed from a protolith extracted from the mantle at ca. >3.8 to 3.5 Ga. Phase 2 (ca. 3.37 to 3.27 Ga) and Phase 3 (ca. 3.19 to 3.14 Ga) record mixed magma sources, with juvenile input during each phase. Evolving oxygen isotope signatures reflect both an increase in the incorporation of sediments, and an elevation of the oxygen isotope signature of those sediments; critically, these result from increases in crustal thickening and continental emergence, respectively. No apparent geodynamic change is recorded by whole-rock geochemistry; our preferred interpretation is that all phases formed in a subduction-related setting, and that crustal thickening was assisted by increasing strength of the lithosphere. The timing of continental emergence of the Coorg Block is similar to that recorded by the Pilbara Craton, but may not be representative of the global record. As such, detailed magmatic records from each craton are needed to further understand the evolution of the Earth's continental crust (as well as to ground-truth numerical models), rather than relying on detrital datasets alone.

Acknowledgements

N.R. publishes with permission of the Executive Director of the British Geological Survey. M.S. was supported by Foreign Expert research grants from China University of Geosciences Beijing, China and Professorial position at the University of Adelaide, Australia. We thank two reviewers for their insightful comments that allowed us to significantly improve the manuscript. All supporting data are included as two tables in the supporting information, along with an accompanying explanation file.

References

Amaldev, T., Santosh, M., Tang, L., Baiju, K.R., Tsunogae, T. and Satyanarayanan, M., 2016. Mesoarchean convergent margin processes and crustal evolution: Petrologic, geochemical and zircon U–Pb and Lu–Hf data from the Mercara Suture Zone, southern India. *Gondwana Research*, *37*, 182-204.

Bindeman, I.N., Bekker, A. and Zakharov, D.O., 2016. Oxygen isotope perspective on crustal evolution on early Earth: A record of Precambrian shales with emphasis on Paleoproterozoic glaciations and Great Oxygenation Event. *Earth and Planetary Science Letters*, *437*, 101-113.

Bouvier, A., Vervoort, J.D. and Patchett, P.J., 2008. The Lu–Hf and Sm–Nd isotopic composition of CHUR: constraints from unequilibrated chondrites and implications for the bulk composition of terrestrial planets. *Earth and Planetary Science Letters*, *273*, 48-57.

Cavosie, A.J., Valley, J.W. and Wilde, S.A., 2005. Magmatic δ18O in 4400–3900 Ma detrital zircons: A record of the alteration and recycling of crust in the Early Archean. *Earth and Planetary Science Letters*, *235*, 663-681.

Chetty, T.R.K., Mohanty, D.P., Yellappa, T., 2012. Mapping of shear zones in the Western Ghats, Southwestern part of Dharwar Craton. *Journal of the Geological Society of India, 79*, 151-154.

Chiaradia, M., 2015. Crustal thickness control on Sr/Y signatures of recent arc magmas: an Earth scale perspective. *Scientific reports*, *5*, 8115. doi:10.1038/scirep08115.

Condie, K.C., 2016. A planet in transition: The onset of plate tectonics on Earth between 3 and 2 Ga?. *Geoscience Frontiers, 9*, 52-60.

Dhuime, B., Hawkesworth, C.J., Cawood, P.A. and Storey, C.D., 2012. A change in the geodynamics of continental growth 3 billion years ago. *Science*, *335*, 1334-1336.

Dhuime, B., Wuestefeld, A. and Hawkesworth, C.J., 2015. Emergence of modern continental crust about 3 billion years ago. *Nature Geoscience*, *8*, 552.

Fielding, L., Najman, Y., Millar, I., Butterworth, P., Ando, S., Padoan, M., Barfod, D. and Kneller, B., 2017. A detrital record of the Nile River and its catchment. *Journal of the Geological Society*, *174*, 301-317.

Fischer, R. and Gerya, T., 2016. Regimes of subduction and lithospheric dynamics in the Precambrian: 3D thermomechanical modelling. *Gondwana Research*, *37*, 53-70.

Fisher, C.M. and Vervoort, J.D., 2018. Using the magmatic record to constrain the growth of continental crust—The Eoarchean zircon Hf record of Greenland. *Earth and Planetary Science Letters*, *488*, 79-91.

Flament, N., Coltice, N. and Rey, P.F., 2008. A case for late-Archaean continental emergence from thermal evolution models and hypsometry. *Earth and Planetary Science Letters*, *275*, 326-336.

Gardiner, N.J., Johnson, T.E., Kirkland, C.L. and Smithies, R.H., 2018. Melting controls on the lutetium–hafnium evolution of Archaean crust. *Precambrian Research*, *305*, 479-488.

Ge, R., Zhu, W., Wilde, S.A. and He, J., 2014. Zircon U–Pb–Lu–Hf–O isotopic evidence for≥ 3.5 Ga crustal growth, reworking and differentiation in the northern Tarim Craton. *Precambrian Research*, *249*, 115-128.

Griffin, W.L., Pearson, N.J., Belousova, E., Jackson, S.E., Van Achterbergh, E., O'Reilly, S.Y. and Shee, S.R., 2000. The Hf isotope composition of cratonic mantle: LAM-MC-ICPMS analysis of zircon megacrysts in kimberlites. *Geochimica et Cosmochimica Acta*, *64*, 133-147.

Harrison, T.M., 2009. The Hadean crust: evidence from> 4 Ga zircons. *Annual Review of Earth and Planetary Sciences*, *37*, 479-505.

Hawkesworth, C., Cawood, P.A. and Dhuime, B., 2018. Rates of generation and growth of the continental crust. *Geoscience Frontiers, in press.* doi:10.1016/j.gsf.2018.02.004

Herzberg, C., Condie, K. and Korenaga, J., 2010. Thermal history of the Earth and its petrological expression. *Earth and Planetary Science Letters*, *292*, 79-88.

Jayananda, M., Chardon, D., Peucat, -J.-J., and Fanning, C.M., 2015, Paleo- to Mesoarchean TTG accretion and continental growth, western Dharwar craton, southern India: SHRIMP U-Pb zircon geochronology, whole-rock geochemistry and Nd-Sr isotopes: *Precambrian Research, 268*, 295–322.

Jayananda, M., Santosh, M. and Aadhiseshan, K.R., 2018. Formation of Archean (3600–2500 Ma) continental crust in the Dharwar Craton, southern India. *Earth-Science Reviews*, *181*, 12-42.

Johnson, T.E., Brown, M., Gardiner, N.J., Kirkland, C.L. and Smithies, R.H., 2017. Earth's first stable continents did not form by subduction. *Nature*, *543*, 239.

Lee, C.T.A., Caves, J., Jiang, H., Cao, W., Lenardic, A., McKenzie, N.R., Shorttle, O., Yin, Q.Z. and Dyer, B., 2018. Deep mantle roots and continental emergence: implications for whole-Earth elemental cycling, long-term climate, and the Cambrian 450 explosion. *International Geology Review*, *60*, 431-448.

Li, Z.X., Li, X.H., Wartho, J.A., Clark, C., Li, W.X., Zhang, C.L. and Bao, C., 2010a. Magmatic and metamorphic events during the early Paleozoic Wuyi-Yunkai orogeny, southeastern South China: New age constraints and pressure-temperature conditions. *Bulletin*, *122*, 772-793.

Li, X.H., Long, W.G., Li, Q.L., Liu, Y., Zheng, Y.F., Yang, Y.H., Chamberlain, K.R., Wan, D.F., Guo, C.H., Wang, X.C. and Tao, H., 2010b. Penglai zircon megacrysts: a potential new working reference material for microbeam determination of Hf–O isotopes and U–Pb age. *Geostandards and Geoanalytical Research*, *34*, 117-134.

Mantle, G.W. and Collins, W.J., 2008. Quantifying crustal thickness variations in evolving orogens: Correlation between arc basalt composition and Moho depth. *Geology*, *36*, 87-90.

Maruyama, S. and Ebisuzaki, T., 2017. Origin of the Earth: a proposal of new model called ABEL. *Geoscience Frontiers*, *8*, 253-274.

Moyen, J.F., 2011. The composite Archaean grey gneisses: petrological significance, and evidence for a non-unique tectonic setting for Archaean crustal growth. *Lithos*, *123*(1-4), pp.21-36.

Moyen, J.F. and Laurent, O., 2017. Archaean tectonic systems: A view from igneous rocks. Lithos, in press. DOI:10.1016/j.lithos.2017.11.038.

Nagel, T.J., Hoffmann, J.E. and Münker, C., 2012. Generation of Eoarchean tonalite-trondhjemite-granodiorite series from thickened mafic arc crust. *Geology*, *40*, 375-378.

Næraa, T., Scherstén, A., Rosing, M.T., Kemp, A.I.S., Hoffmann, J.E., Kokfelt, T.F. and Whitehouse, M.J., 2012. Hafnium isotope evidence for a transition in the dynamics of continental growth 3.2 Gyr ago. *Nature*, *485*, 627.

Payne, J.L., Hand, M., Pearson, N.J., Barovich, K.M. and McInerney, D.J., 2015. Crustal thickening and clay: Controls on O isotope variation in global magmatism and siliciclastic sedimentary rocks. *Earth and Planetary Science Letters*, *412*, 70-76.

Peucat, J-J., Jayananda, M. Chardon, D., Capdevila, R., Fanning Marc. C., Paquette, Jean-Louis., 2013. The lower crust of Dharwar craton, south India: Patchwork of 469 Archean granulitic domains. *Precambrian Research, 227*, 4-29.

Pons, M.L., Fujii, T., Rosing, M., Quitté, G., Télouk, P. and Albarède, F., 2013. A Zn isotope perspective on the rise of continents. *Geobiology*, *11*, 201-214.

Profeta, L., Ducea, M.N., Chapman, J.B., Paterson, S.R., Gonzales, S.M.H., Kirsch, M., Petrescu, L. and DeCelles, P.G., 2015. Quantifying crustal thickness over time in magmatic arcs. *Scientific Reports*, *5*, 17786.

Rey, P.F. and Coltice, N., 2008. Neoarchean lithospheric strengthening and the coupling of Earth's geochemical reservoirs. *Geology*, *36*, 635-638.

Roberts, N.M.W. and Spencer, C.J., 2015. The zircon archive of continent formation through time. In: Roberts, N.M.W., Van Kranendonk, M., Parman, S., Shirey, S. & Clift, P.D. (eds) Continent formation through time. *Geological Society, London,* 491 *Special Publications, 389*, 197-225.

Roberts, N.M., Yang, Q.Y. and Santosh, M., 2018. Rapid oxygen diffusion during high temperature alteration of zircon. *Scientific reports*, *8*, 3661.

Rozel, A.B., Golabek, G.J., Jain, C., Tackley, P.J. and Gerya, T., 2017. Continental crust formation on early Earth controlled by intrusive magmatism. *Nature*, *545*, 332.

Rubatto, D., 2017. Zircon: the metamorphic mineral. *Reviews in mineralogy and geochemistry*, *83*, 261-295.

Santosh, M., Yang, Q-Y., Shaji, E., Tsunogae, T., Ram Mohan, M., Satyanarayanan, M., 2015. An exotic Mesoarchean microcontinent: The Coorg Block, southern India. *Gondwana Research, 27*, 165-195.

Santosh, M., Yang, Q-Y., Shaji, E., Ram Mohan, M., Tsunogae, T., Satyanarayanan, M., 2016. Oldest rocks from Peninsular India: Evidence for Hadean to Neoarchean crustal evolution. *Gondwana Research, 29*, 105-135.

Sizova, E., Gerya, T., Brown, M. and Perchuk, L.L., 2010. Subduction styles in the Precambrian: Insight from numerical experiments. *Lithos*, *116*, 209-229.

Spencer, C.J., Roberts, N.M., Cawood, P.A., Hawkesworth, C.J., Prave, A.R., Antonini, A.S. and Horstwood, M.S., 2014. Intermontane basins and bimodal volcanism at the onset of the Sveconorwegian Orogeny, southern Norway. *Precambrian Research*, *252*, 107-118.

Spencer, C.J., Roberts, N.M.W. and Santosh, M., 2017. Growth, destruction, and preservation of Earth's continental crust. *Earth-Science Reviews*, *172*, 87-106.

Stern, R.J., 2008. Modern-style plate tectonics began in Neoproterozoic time: An alternative interpretation of Earth's tectonic history. *When did plate tectonics begin on planet Earth*, *440*, 265-280.

Sun, S.S. and McDonough, W.S., 1989. Chemical and isotopic systematics of oceanic basalts: implications for mantle composition and processes. In: Saunders, A.D. & Norry, M.J. (eds). Magmatism in the Ocean Basins. *Geological Society, London, Special Publications*, *42*, 313-345.

Szilas, K., Maher, K. and Bird, D.K., 2016. Aluminous gneiss derived by weathering of basaltic source rocks in the Neoarchean Storø Supracrustal Belt, southern West Greenland. *Chemical Geology*, *441*, 63-80.

Tang, M., Wang, X.L., Shu, X.J., Wang, D., Yang, T. and Gopon, P., 2014. Hafnium isotopic heterogeneity in zircons from granitic rocks: Geochemical evaluation and modeling of "zircon effect" in crustal anatexis. *Earth and Planetary Science Letters*, *389*, pp.188-199.

Valley, J.W., 2003. Oxygen isotopes in zircon. *Reviews in mineralogy and geochemistry*, *53*, 343-385.

Valley, J.W., Kinny, P.D., Schulze, D.J. and Spicuzza, M.J., 1998. Zircon megacrysts from kimberlite: oxygen isotope variability among mantle melts. *Contributions to mineralogy and petrology*, *133*, 1-11.

Van Kranendonk, M.J., 2010. Two types of Archean continental crust: Plume and plate tectonics on early Earth. *American Journal of Science*, *310*, 1187-1209.

Van Kranendonk, M.J., Kirkland, C.L. and Cliff, J., 2015. Oxygen isotopes in Pilbara Craton zircons support a global increase in crustal recycling at 3.2 Ga. *Lithos*, *228*, 90-98.

Vlaar, N.J., 2000. Continental emergence and growth on a cooling earth. *Tectonophysics*, *322*, 191-202.

Wang, D., Wang, X.L., Cai, Y., Goldstein, S.L. and Yang, T., 2018. Do Hf isotopes in magmatic zircons represent those of their host rocks?. *Journal of Asian Earth Sciences*, *154*, 202-212.

Whitehouse, M.J., Nemchin, A.A. and Pidgeon, R.T., 2017. What can Hadean detrital zircon really tell us? A critical evaluation of their geochronology with implications for the interpretation of oxygen and hafnium isotopes. *Gondwana Research*, *51*, 78-91.

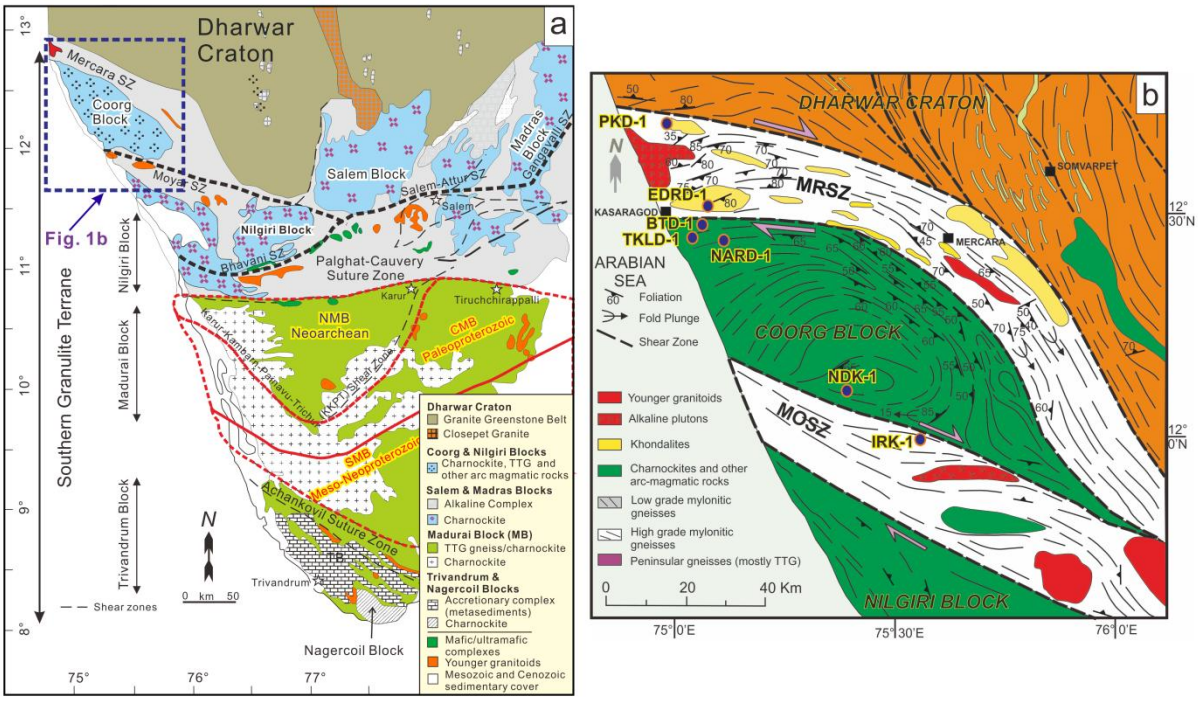

Figure 1 (a) Generalised geological and tectonic framework of the Southern Granulite Terrane of India showing the major crustal blocks and intervening suture zones (after Santosh et al., 2016 and references therein). (b) Geological map of the Coorg Block and surrounding suture zones (modified from Chetty et al., 2013, *Jour. Geol. Soc. India*, 72, 151–154; with permission from Geological Society of India, Bengaluru), showing the sample locations.

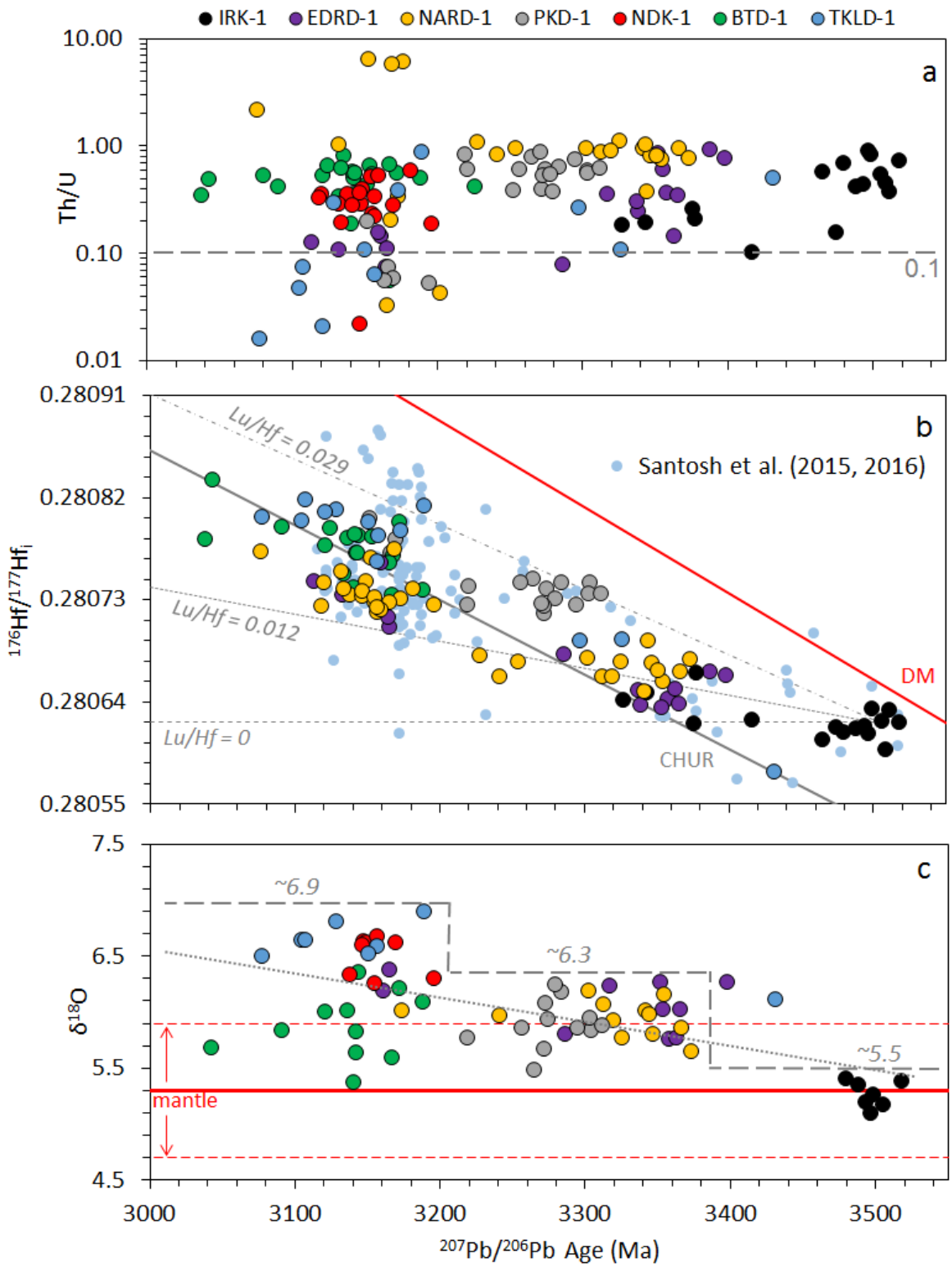

Figure 2 (a) Zircon Th/U ratio plotted versus corresponding $^{207}Pb/^{206}Pb$ spot age. The 0.1 line representing magmatic vs. metamorphic compositions is shown (see Rubatto, 2017). (b) Initial $^{176}Hf/^{177}Hf$ ratio versus zircon $^{207}Pb/^{206}Pb$ spot age. Depleted mantle (DM; after Griffin et al., 2000) and CHUR after Bouvier et al. (2008) are shown, along with evolution trends from sample IRK-1 for Lu/Hf = 0, 0.012 and 0.029 (see text for explanation; dashed grey

lines). (c) Zircon $\delta^{18}O_{VSMOW}$ plotted versus their corresponding $^{207}Pb/^{206}Pb$ spot. The mantle mean and range for zircon of Valley et al. (1998) is shown (solid and dashed red lines), as is the secular increase in maximum zircon values of this study through each phase of magmatism via an interpreted step-change (dashed grey line) and best-fit line (dotted grey line).

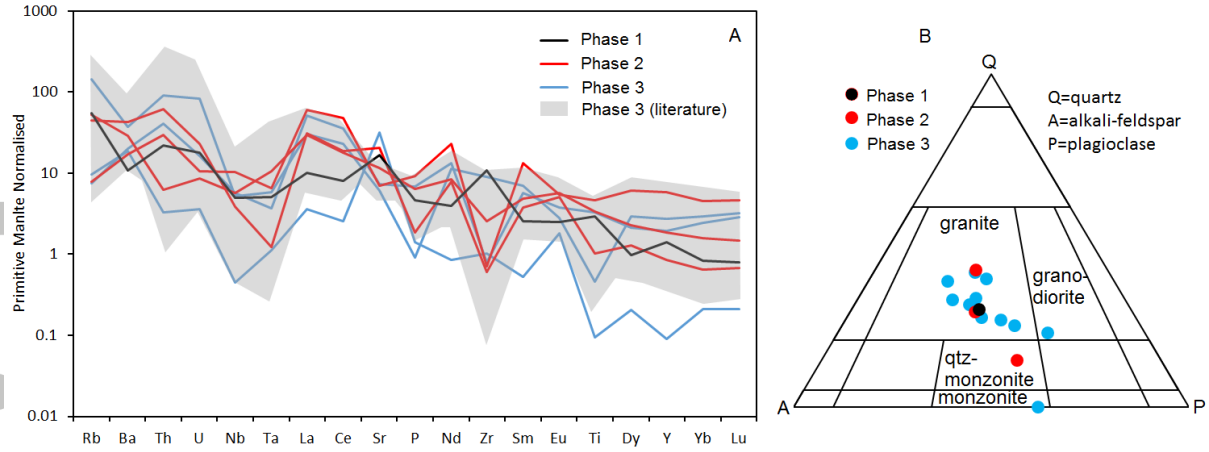

Figure 3 Primitive mantle (Sun & McDonough, 1989) normalised plot of whole-rock geochemistry; data from Santosh et al., (2015 and 2016), literature = samples not included in this study.

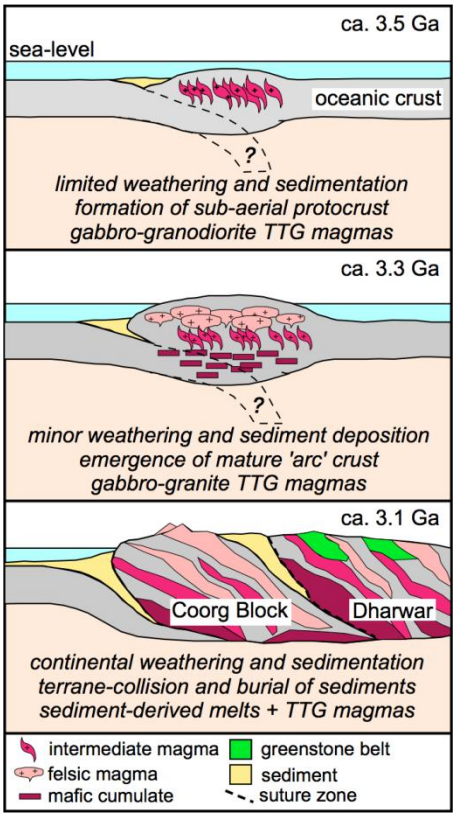

Figure 4 Cartoon tectonic model highlighting the key changes in continental composition during each magmatic phase. It should be noted that the behaviour of subducting lithosphere versus upwelling mantle is speculative for Archean tectonics, and thus we place little emphasis on this aspect of the model. Our preferred model is that of horizontal tectonics and plate boundary convergence being responsible for magmatism, rather than a rising plume.

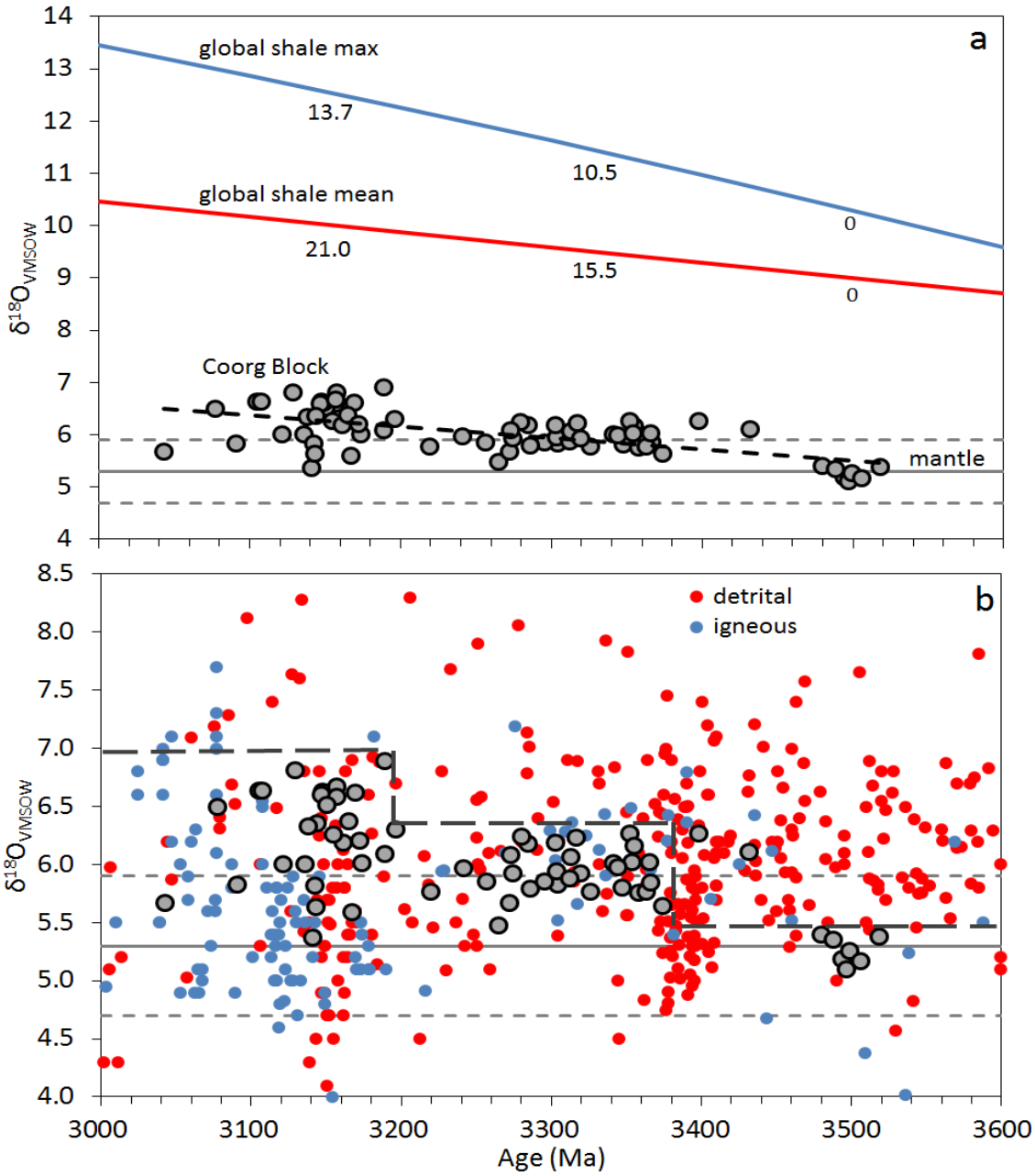

Figure 5 (a) Zircon $\delta^{18}O$ and correlative $^{207}Pb/^{206}Pb$ spot ages of Coorg Block rocks (grey circles), compared with the trends of global shale database, both mean and maximum (from Bindeman et al., 2016). The results of two-component mixture modelling are shown for each magmatic stage adjacent to the crustal (shale) component modelled. Mantle range after Valley et al. (1998). (b) Zircon $\delta^{18}O$ and correlative $^{207}Pb/^{206}Pb$ spot ages of Coorg Block rocks (grey circles), compared with literature data from igneous (blue) and detrital (red) zircons (database of Spencer et al., 2017). Thick dashed grey line represents the secular increase recorded in the Coorg Block maximum values.